Clay Minerals, (2018) **53**, 447–457

Characterization of clays from the Foumban region (west Cameroon) and evaluation for refractory brick manufacture

A. POUNTOUENCHI[1,*], D. NJOYA[1], A. NJOYA[2], D. RABIBISAO[3], J.R. MACHE[4], R.F. YONGUE[5], D. NJOPWOUO[1], N. FAGEL[6], P. PILATE[7] AND L. VAN PARYS[8]

[1] *Department of Inorganic Chemistry, Faculty of Science, University of Yaoundé I, 812, Yaoundé, Cameroon*
[2] *Department of Arts, Technology and Heritage, Institute of Fine Arts of Foumban, University of Dschang 31, Foumban, Cameroon*
[3] *Material Department, Higher Polytechnique School, 101, Antananarivo, Madagascar.*
[4] *MIPROMALO, Yaoundé, Cameroon*
[5] *Department of Earth Sciences, University of Yaoundé I, 812, Yaoundé, Cameroon*
[6] *AGEs, Department of Geology, University of Liege, Allée du six août, 14, Liege, Belgium*
[7] *Belgian Ceramic Research Centre, Governor Cornez avenue 4, 7000, Mons, Belgium*
[8] *Materials Research Institute, University of Mons, Place du parc 2, 7000, Mons, Belgium*

(*Received 25 September 2017; revised 16 June 2018; Guest Associate Editor: Michele Dondi*)

ABSTRACT: Three clayey materials named MY3, KK and KG originating from the Foumban region (west Cameroon) were analysed to determine their granulometry, plasticity, major-element chemistry and mineralogy. Dilatometric and ceramic behaviour were also investigated. Clays were shaped by uniaxial pressing in a steel mould. Shaped samples were heated at 1300, 1400 and 1500°C. The end products were characterized in terms of their density, porosity and compressive strength. Raw materials differ in terms of their mineralogical composition, grain-size distribution, Al_2O_3 content and the nature and abundance of impurities inducing specific thermal behaviour during dilatometric analysis and sintering tests. The final material properties may be related to the main features of the raw materials used.

KEYWORDS: clay, analysis, refractory materials, optical microscopy, chemical properties, Cameroon.

Refractory (ceramic) materials are materials other than metals and alloys (but not excluding those with a metallic constituent) that are physically and chemically stable up to at least 1500°C (Jourdain, 1966; Kolli *et al*., 2007; Porier, 2011). Based on the chemical and mineralogical composition of the initial raw materials, refractories are classified into three main groups, namely: acid refractories (Al refractories, Si refractories and Al–Si refractories), basic refractories (mainly magnesia, dolomite and chromite refractories) and special refractories (carbons, carbides, nitrides, spinel, zircon) (Aliprandi, 1979; Lapoujade & Le Mat, 1986; Staphen & Gordon, 1992; Routschka, 2004; Amrane *et al*., 2011). The Al–Si refractories are numerous and have many applications (Routschka, 2004). They are used in metallurgy, ceramics and glass industries. Fireclay refractories are manufactured from natural

This paper was originally presented during the session: 'CZ-01 – Clays for ceramics' of the International Clay Conference 2017.
*E-mail: apountouenchi@uy1.uninet.cm
https://doi.org/10.1180/clm.2018.32

clay materials. Their cost of fabrication is relatively small compared to other bricks manufactured from synthetic materials (Lapoujade & Le Mat, 1986). Fireclays might be used as building materials for furnaces, vessels and reactors for various applications such as fabrication of pottery, earthenware, cement for metallurgy, etc.

In addition, they are produced by mixing fine raw clay particles (bonding phase) with large particles (aggregates) referred to as chamotte particles. Chamotte is obtained by pre-firing raw clays, grinding, sieving and classifying grains to obtain particle-size distributions of 0.5 to several millimetres. Previous studies have characterized fireclay refractory bricks from some Cameroonian raw materials (Djangang *et al*., 2007, 2008, 2010; Tchamba *et al*., 2011). The present study focused on the characterization of clays of the Koutaba and Mayouom deposits and their assessment for the production of refractory bricks. Knowledge of the thermal behaviour of clays is necessary both for chamotte fabrication and for their use as a bonding phase in final materials, and it is a prerequisite for further developments.

MATERIALS AND METHODS

The samples investigated are from two clay deposits in west Cameroon: Koutaba (KK-white and KG-greyish)

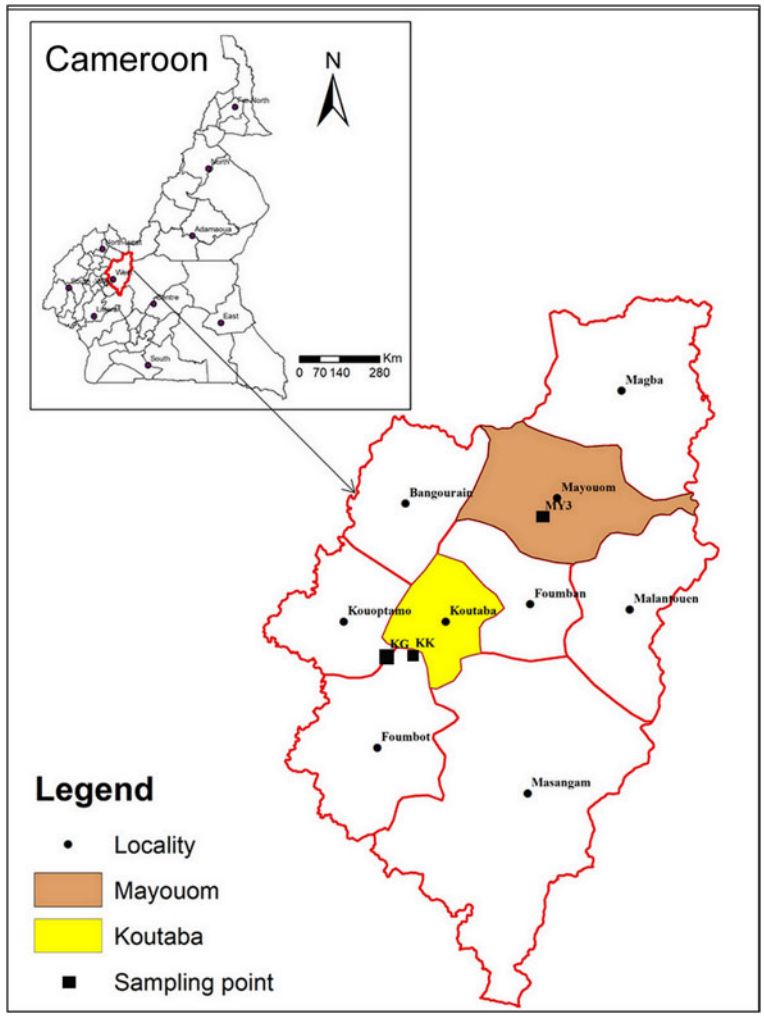

Fig. 1. Map of Cameroon showing the locations of the materials studied (after Nkalih, 2016).

https://doi.org/10.1180/clm.2018.32 Published online by Cambridge University Press

and Mayouom (MY3-white). Koutaba is situated ~20 km south of Foumban at 5°35′ north latitude and 10°41′ east longitude. Mayouom is ~30 km north of Foumban at 5°51′ north latitude and 10°59′ east longitude (Fig. 1). The clayey materials KK and MY3 are of residual origin and result from the alteration of granites (Nkalih *et al*., 2015) and mylonites (Njoya, 2007), respectively. KG is a hydromorphic clay found in a large alluvial plain (Nkalih *et al*., 2015). The selection of these deposits was based on previous studies that indicated their sufficient extent for industrial exploitation (Njoya *et al*., 2006; Njoya, 2007; Tassongwa *et al*., 2014; Nkalih *et al*., 2015). These sites are also attractive due to their good road access.

The raw clays were sampled at various depths from 0.3 to 1.8 m using hand augers. They were oven dried until they reached constant mass at 110°C, ground manually and sieved at 100 µm.

The chemical composition was determined by X-ray fluorescence (XRF). Samples were prepared by fusion with lithium tetraborate and lithium bromide in platinum crucibles (Bennett *et al*., 1976) and casted to form glass beads. The analysis of the mineralogical phases was performed by X-ray diffraction (Bruker D8 Advance diffractometer) using monochromatic Cu-*K*α radiation (l = 1.5406 Å) over the range 2–70°2θ in steps of 0.020° operated at 40 kV and 25 mA (Reynolds & Moore, 1989).

The particle-size analysis of the samples was performed at the Laboratory of Geotechnologies at the University of Yaoundé I. The samples were dry-sieved to obtain the ≥100 µm fraction. The fraction of <100 µm was obtained by gravity sedimentation according to Stoke's law. Plasticity was characterized by the Atterberg limits (plastic limit [PL], liquid limit [LL] and plasticity index [PI]) determined with the Casagrande method (American Society for Testing Materials [ASTM] norm D-4318).

The thermal linear expansion was measured on pressed cylindrical clay samples with a connecting rod dilatometer. Specimens were heated from 20 to 1400°C for KK and from 20 to 1300°C for MY3 and KG at 5°C/min heating and cooling rates. To investigate the thermal behaviour of the samples, 3 cm × 3 cm cylindrical specimens were pressed uniaxially at 42 MPa using a hydraulic press. These specimens were fired at 1300, 1400 and 1500°C for 4 h in an electric furnace with heating and cooling rates of 5°C/min.

The fired products were characterized by their linear shrinkage (El Yacoubi *et al*., 2006), their bulk density, water absorption, open porosity and compressive strength, and by phase analysis. Bulk density, water absorption and open porosity were determined using the hydrostatic method (Seynou *et al*., 2013). Compressive strength was calculated from the maximum load obtained during a test on fired products using a hydraulic press.

The mineralogical composition of fired products sintered at 1300 to 1500°C was determined by XRD using a Philips PW 1729 diffractometer operating at 40 kV, 40 mA using graphite monochromatic Cu-*K*α radiation. The XRD patterns were treated with *CRYSTAL* software to determine the mineralogy. The microstructure was determined on the polished surface of fired products with optical microscopy.

RESULTS AND DISCUSSION

Raw material characterization

Chemical composition. The chemical compositions of the samples are listed in Table 1. Sample KK is richest in SiO_2 and poorest in Al_2O_3, whereas samples KG and MY3 have similar SiO_2 and Al_2O_3 contents. The presence of fluxing agent such as TiO_2, Fe_2O_3, alkalis, CaO and MgO may contribute to decrease of the melting temperature and increase in the appearance of vitreous phases. The large SiO_2 content in sample KK is due to the large sand fraction (Table 1). The Al_2O_3 content ranges between 10% and 30% and the SiO_2 content is <85%. Therefore, KK, KG and MY3 may be considered

Table 1. Chemical composition (wt.%) of the clays.

Sample	LOI	SiO_2	Al_2O_3	Fe_2O_3	MnO	MgO	CaO	Na_2O	K_2O	TiO_2	Total
KK	5.4	77.3	15.6	0.8	0.01	0.0	0.2	bdl	0.7	0.1	100.0
KG	10.6	57.6	26.1	3.1	0.01	0.3	0.3	bdl	0.3	1.4	99.7
MY3	10.2	58.5	28.1	0.5	0.00	0.1	0.1	bdl	0.9	1.3	98.7

bdl = below detection limit; LOI = loss on ignition.

https://doi.org/10.1180/clm.2018.32 Published online by Cambridge University Press

for manufacturing low-alumina fireclay refractory materials (LF10 group) (ISO 10081-1, 2003).

Mineralogy. The XRD traces of the KK, KG and MY3 clays are shown in Fig. 2. Sample KK consists mainly of kaolinite, illite, quartz and goethite. The high quartz content is in good agreement with the particle-size distribution and chemical analyses. Sample KG contains kaolinite, quartz, montmorillonite and anatase as the main phases. The presence of montmorillonite explains the high plasticity of this clay. MY3 consists of kaolinite, quartz, illite, goethite and anatase. The presence of anatase in KG and MY3 is in good agreement with the TiO_2 content (Table 1). In summary, the three materials contain kaolinite associated with illite or montmorillonite and quartz.

Particle-size distribution and plasticity. The particle size distribution of the raw materials is listed in Table 2. The silt fraction predominates in the clayey materials KK and MY3, whereas clay fraction predominates in KG. Specimen KK has the largest sandy fraction and the smallest clay fraction.

Table 3 lists the results of the Atterberg limits (PL, PP and PI) of the three samples. KK has the smallest PL and LL values of the three samples; hence, it requires a smaller water content to be plastic and to flow without external force. PI corresponds to the water content of a clay necessary to allow it to be plastic: the more plastic the clay, the more water that is retained without the clay becoming fluid (Jouenne, 1984). The PI of the KG clay (39%) is very large compared to those of MY3 (18%) and KK (7%). The PI is linked to the clay-mineral content (Kornmann & Ingénieurs du Centre Technique des Tuiles et Briques, 2005).

Plasticity is an important parameter in industrial processes. After mixing with large chamotte grains, raw clay only acts as the bonding phase of the materials and only small quantities of water may be added for the classical dry-pressing method. Plasticity is necessary for the extrusion process of fabrication. A high plasticity allows the clay to lubricate and facilitate displacement and densification of the chamotte particles and to reduce friction along the steel mould. This parameter was not investigated in the present laboratory work. In industrial practice, KG clay might be used to increase the plasticity of the raw material mixtures, if necessary.

Thermo-dilatometric analysis. Figure 3 displays the dilatometric curves of the three clays. Up to 500°C, the three clays exhibit a small expansion due to the thermal activation associated with heating. Sample KK exhibits expansion at temperatures of >575°C, whereas samples MY3 and KG exhibit sharp shrinkages between 575 and 600°C. The KK expansion may be explained by the $\alpha \rightarrow \beta$ quartz phase transition associated with a large volume expansion. The greater quartz content and the smaller clay-mineral content of this sample is in accord with this interpretation. The shrinkage of MY3 and KG is explained by the dehydroxylation of kaolinite, which results in metakaolinite formation (Djangang *et al*., 2010; Bakr, 2011; Zerbo *et al*., 2012; Sadik *et al*., 2014).

The next sharp shrinkage was observed at between 900 and 975°C in the KG and MY3 samples and is related to the breakdown of metakaolinite and the reorganization of the system (Ribeiro *et al*., 2005; Pialy *et al*., 2009). The intensity of this event may be related to the clay-mineral content. It is larger for the KG sample than for the MY3 sample.

Above this temperature range, the dilatometric curves (Fig. 3) exhibit a small negative slope, which may be related to a slow sintering associated with shrinkage. At 1000°C (KG) and 1050°C (MY3), the curves indicate a sharp shrinkage indicating acceleration of sintering. The KK sample exhibits greater refractoriness because the sharp shrinkage appears at ~1200°C. Sintering is due to solid and/or liquid diffusion. At lower temperatures, sintering is mainly due to solid diffusion and/or a small amount of the liquid phase. At higher temperatures, the sharp shrinkage may be explained by the sudden appearance of a large quantity of the liquid phase, promoting greater diffusion and flowing into the pores. Firing shrinkage is largely controlled by the finer, most 'active' particles: the clay minerals and fluxing agents. Depending on their nature and abundance, they promote the appearance of larger amounts of the liquid phase at high temperatures (Chavez & Johns, 1995). The high refractoriness of the KK sample is due to the large quartz content. Quartz is at the end of the binary Al_2O_3–SiO_2 system phase diagram, with a higher melting temperature than for clay minerals located near the eutectic composition (Lapoujade & Le Mat, 1986).

Fired-product characterization

Physical and mechanical properties of fired products. Figure 4 presents the evolution of the shrinkage, bulk density, water absorption, open porosity and compressive strength *vs*. firing temperature. Samples KG and MY3 exhibit similar behaviour. Shrinkage and bulk

https://doi.org/10.1180/clm.2018.32 Published online by Cambridge University Press

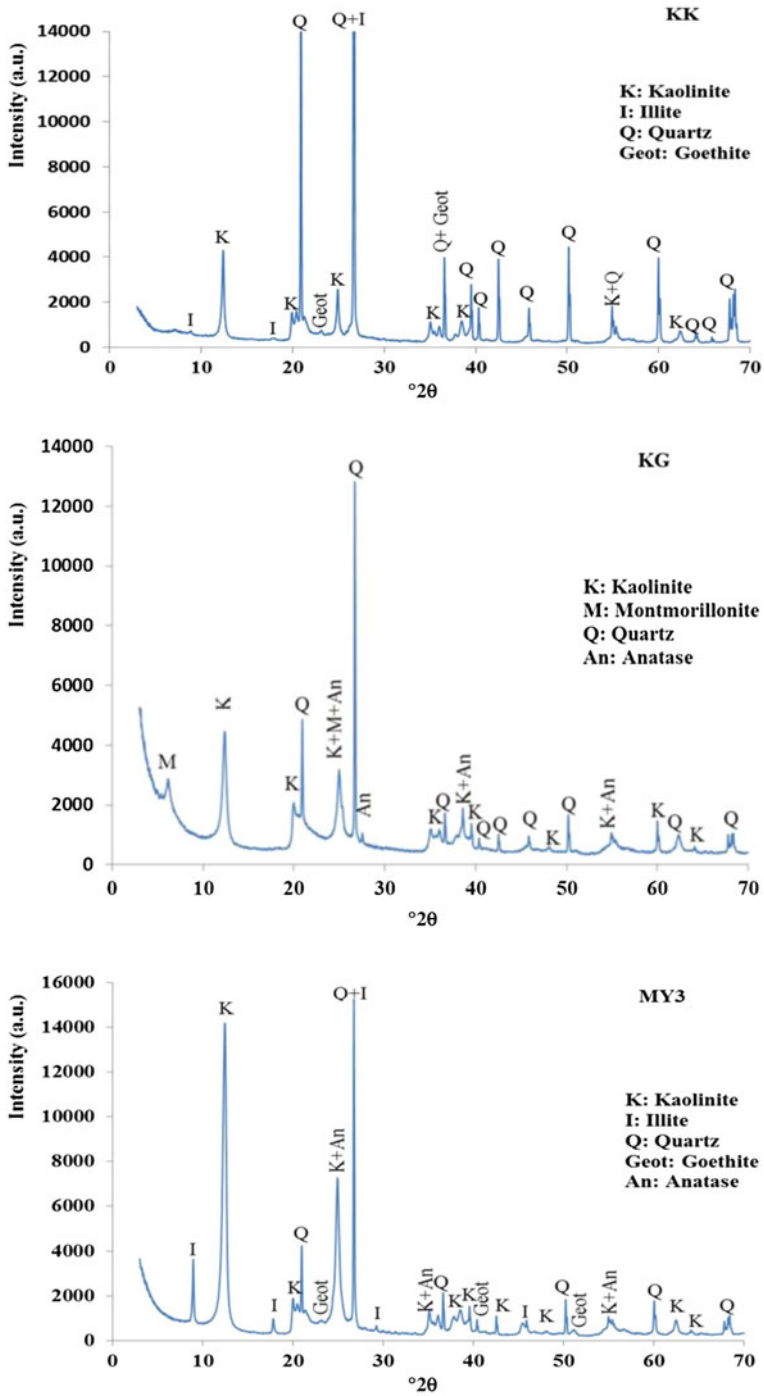

FIG. 2. XRD traces of samples KK, KG and MY3.

https://doi.org/10.1180/clm.2018.32 Published online by Cambridge University Press

TABLE 2. Particle-size distribution of the raw materials.

Sample	Particle diameters (μm) and their percentage mass				
	Clay (≤2)	Fine silt (2–20)	Coarse silt (20–50)	Fine sand (50–200)	Coarse sand (200–2000)
KK	9	37	28	20	6
MY3	23	53	13	10	1
KG	65	10	8	15	2

TABLE 3. Atterberg limits of the clays.

Sample	Liquid limit (%)	Plastic limit (%)	Plasticity index (%)
KK	37	30	7
MY3	57	39	18
KG	75	36	39

density increase (Fig. 4ab), while open porosity and water absorption decrease (Fig. 4cd) in the temperature range 1300–1500°C. As previously explained, this sintering behaviour may be explained by the presence of a large amount of clay and impurities (Tables 1, 2), and the thermal behaviour already observed during the dilatometric analysis.

Densification of sample KG is greater than that of sample MY3 at 1300°C, but the gap between the two samples decreases with increasing temperature. The densification of these materials results from sintering due to induced liquid phases and from mullite crystallization and SiO_2 phase transformation (quartz to cristobalite) with volume changes (Figs 4, 5). At 1500°C, the two materials are fully densified, the density is maximal and the open porosity is minimized. The evolution of the compressive strength of the fired

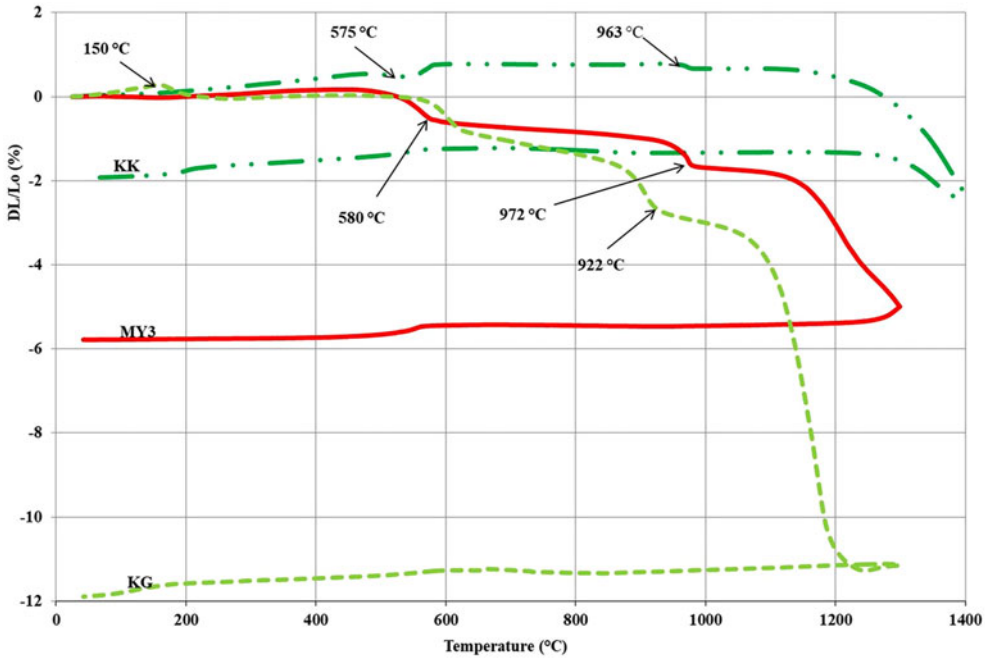

FIG. 3. Dilatometric curves of the clays. Lo = initial length of the brick sample; DL = length of the same sample measured at a specific temperature during firing; DL/Lo = the rate of material expansion/shrinkage.

https://doi.org/10.1180/clm.2018.32 Published online by Cambridge University Press

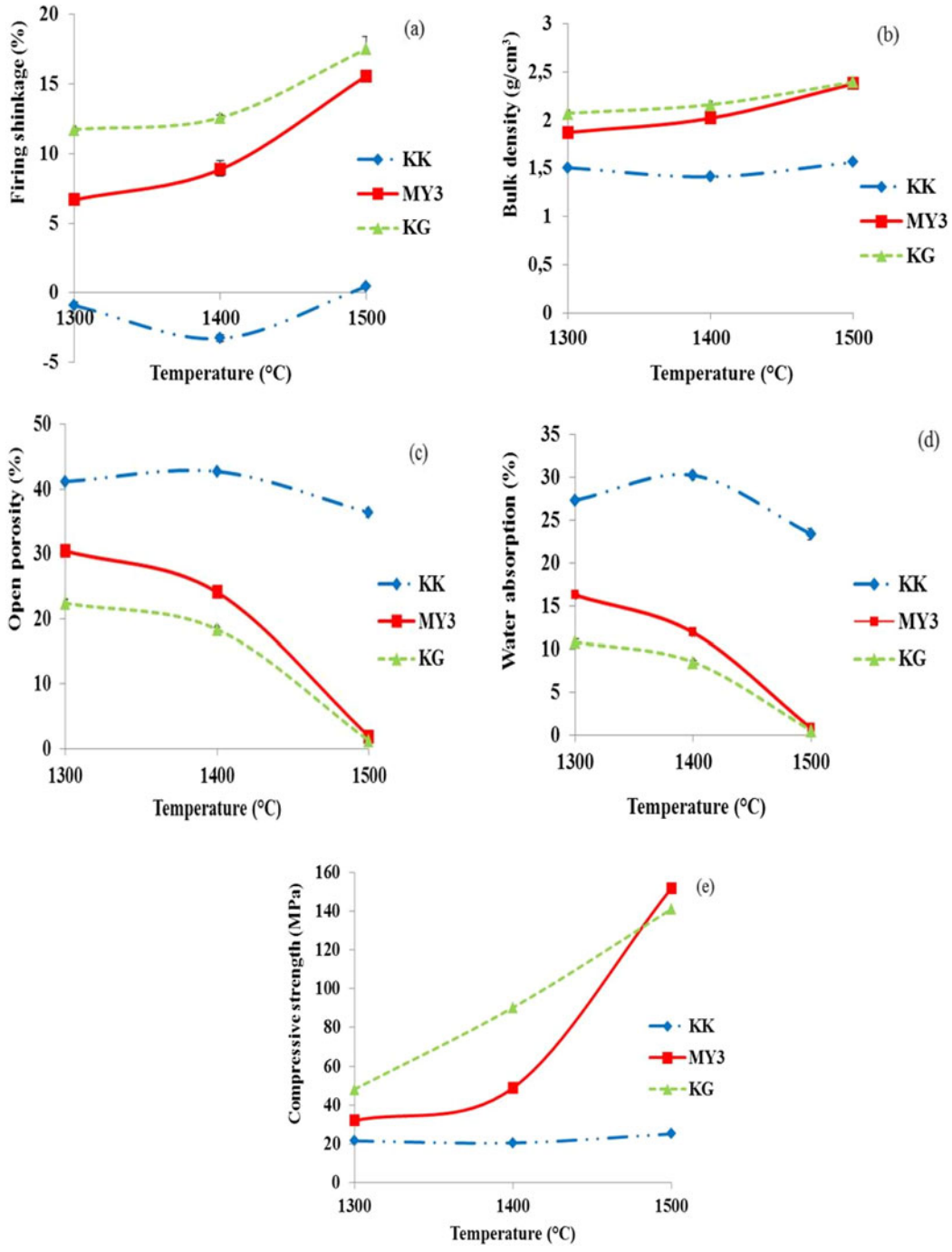

FIG. 4. Densification behaviour of fired products *vs*. temperature: (a) firing shrinkage; (b) bulk density; (c) open porosity; (d) water absorption; and (e) compressive strength.

https://doi.org/10.1180/clm.2018.32 Published online by Cambridge University Press

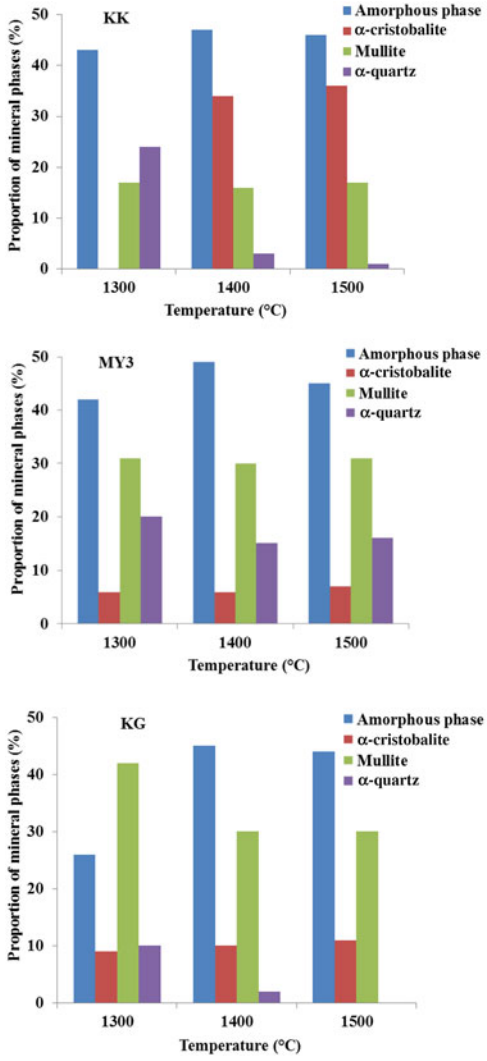

FIG. 5. Semi-quantitative analysis of the fired products *vs.* temperature.

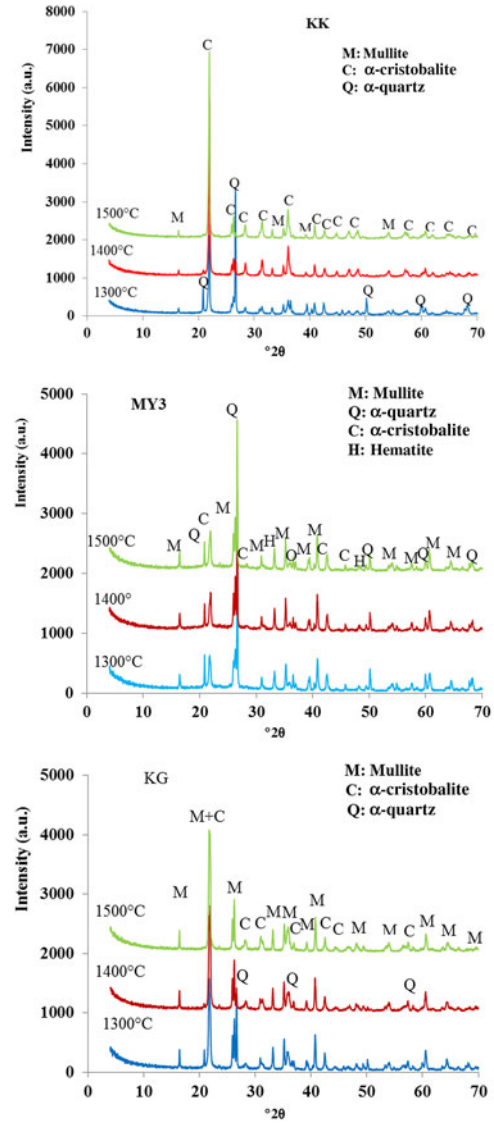

FIG. 6. XRD patterns of the fired bodies.

bodies is similar to the density evolution: it increases with firing temperature, reaching similar values at 1500°C for both clays.

In the temperature range used in this study (1300–1500°C), the KK clay exhibits a small expansion (negative shrinkage) at 1300 and 1400°C, and at 1500°C the shrinkage is almost zero. Density is more or less constant at all temperatures and open porosity values are similar at 1300 and 1400°C. A small decrease is observed at 1500°C. This behaviour may be explained by the small clay and impurity contents (Tables 1, 2), promoting very little of the liquid phase at these firing temperatures. This behaviour may also be explained by the quartz to cristobalite transformation with a 17.4% expansion (Routschka & Wuthnow, 2012), which counterbalances densification.

Overall, the thermal behaviour of the three clays is related to their mineralogical and chemical compositions.

X-ray diffraction of the fired clays. The XRD patterns of the fired bodies are given in Fig. 6 and their semi-

https://doi.org/10.1180/clm.2018.32 Published online by Cambridge University Press

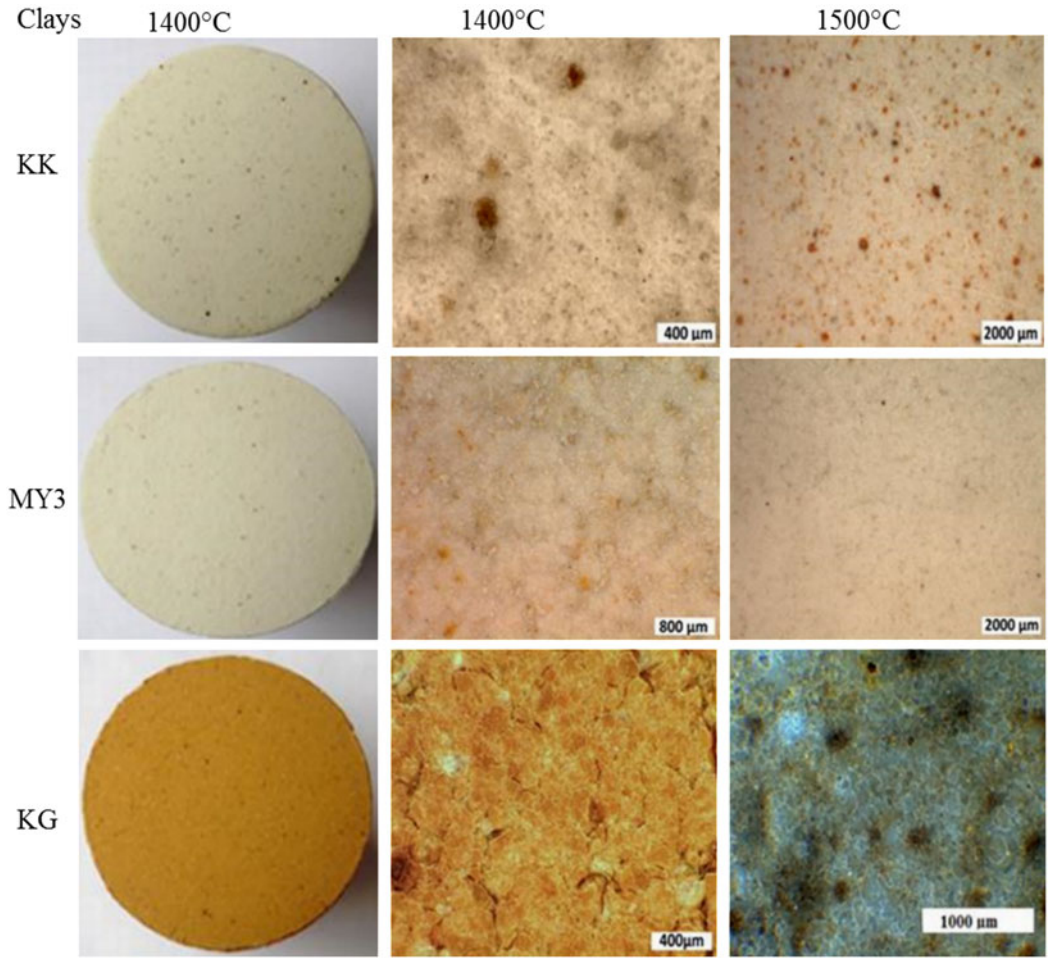

FIG. 7. Photomicrographs of the polished surfaces of the fired products.

quantitative analysis is presented in Fig. 5. All fired materials contain quartz as in the original clays, but they also contain some new phases, namely mullite, cristobalite and amorphous matter. Mullite results from the reaction (Sahnoune *et al*., 2008):

$$3Al_2O_3 + 2SiO_2 \rightarrow 3Al_2O_3.2SiO_2$$

Cristobalite is the result of the quartz transformation at temperatures of >1100°C (Gualtieri & Bertolani, 1992). The amorphous phase results from the melting of impurities at higher temperatures that act as fluxes and promote the melting of silicate phases. Due to the high SiO_2 content, the liquid phase does not crystallize during cooling and a vitreous phase appears, which includes SiO_2, Al_2O_3 and the impurities (Chen *et al*., 2000).

The amount of mullite is proportional to the Al_2O_3 content (Fig. 5; Table 1), which explains the smaller amount of it in sample KK at all temperatures and the similar abundances in samples MY3 and KG at 1400 and 1500°C. In sample KG, the larger amount of mullite at 1300°C is followed by decreases at 1400 and 1500°C, indicating diffusion of Al_2O_3 across a longer distance, dissolution in the amorphous phase and homogenization of the composition. The same behaviour may also hold for longer firing times at 1300°C. For the three clays, the mullite content does not change between 1400 and 1500°C, indicating a full reaction. Therefore, the mullite contents

https://doi.org/10.1180/clm.2018.32 Published online by Cambridge University Press

determined are the maximum ones. The quartz abundance decreases and cristobalite increases with increasing temperature. In samples KK and KG, quartz was not detected at 1400 and 1500°C. In contrast, in sample MY3, quartz is abundant (~15%) at 1400 and 1500°C. The amount of amorphous phase and the temperature of appearance depend on the abundance of Fe_2O_3 and TiO_2 fluxes (Table 1). The three materials contain large amounts of amorphous matter at 1300°C, in good agreement with dilatometric results. The final amounts of amorphous matter (at 1400 and 1500°C) are comparable in all materials. In samples KK and MY3, the abundance of the amorphous phase may be considered constant across the whole temperature range (1300–1500°C), considering the limitations of its determination. In the KG sample, the amorphous phase content varies inversely with mullite between 1300 and 1400°C. This might be explained by a rapid crystallization of mullite from clay particles, followed by the dissolution in the vitreous phase, depending on the kinetic appearance of the latter.

Optical microscopy. Photomicrographs of the fired products at 1400 and 1500°C are shown in Fig. 7. At 1300°C, the material surface is rough due to the low sintering degree and the high residual porosity. At higher temperatures, the polished surfaces are smoother due to densification and porosity closure. During heating, iron diffuses and contributes to the colouration of the final materials. Iron is included in the coloured solid solution and it is also dissolved in a more or less coloured amorphous phase. Hence, iron is the main 'colouring' impurity. Sample MY3, with its smaller Fe_2O_3 content (Table 1), is whiter than its counterparts. Sample KK, with an intermediate Fe_2O_3 content, has some dark spots. Sample KG exhibits a brownish colour due to its large Fe_2O_3 content (Bakr, 2011). The small brown spots in this sample indicate the location of initial goethite particles.

SUMMARY AND CONCLUSIONS

This work is a contribution to the characterization of three clayey raw materials of the Koutaba and Mayouom deposits from west Cameroon and the evaluation of their suitability for use in the preparation of refractory bricks.

The three clays consist of kaolinite and quartz, associated with illite and goethite (KK); montmorillonite and anatase (KG); and illite and anatase (MY3). The clays contain 10–30% Al_2O_3, <85% SiO_2 and 1–3% impurities.

The thermal behaviour of each clay may be related to the abundances of both the clay minerals and the impurities. High levels of clay and impurities promote sintering at low temperatures, and low levels cause densification at higher temperatures.

After heating at 1300–1500°C for 4 h, two resulting materials (KG and MY3) exhibit interesting properties for making bricks, (mainly from 1400°C). The KK sample with the larger SiO_2 content exhibits a small amount of densification even at 1500°C. These materials may be used as raw materials for the manufacture of low-Al_2O_3 refractory materials belonging to the LF10 Group according to ISO 10081-1 (2003).

ACKNOWLEDGMENTS

The authors are grateful to the PAFROID project (Intra-African University Mobility Program) and the ARES (Academy of Research and Higher Education), partner of the Belgian Development Cooperation, for the support given to this study through the PRD project entitled 'Characterization and Valorization of Foumban clays (West Cameroon)'.

REFERENCES

Aliprandi G. (1979) *Matériaux Réfractaires et Céramique Techniques*. Septima, Paris, France.

Amrane B., Ouedraogo E., Mamen B., Djaknoun S. & Mesrati N. (2011) Experimental study of thermo-mechanical behaviour of alumina–silicate refractory materials based on a mixture of Algerian kaolinitic clays. *Ceramics International*, **37**, 3217–3227.

Bakr I.M. (2011) Densification behavior, phase transformations, microstructure and mechanical properties of fired Egyptian kaolins. *Applied Clay Science*, **52**, 333–337.

Bennett H. & Oliver G.J. (1976) Development of fluxes for the analysis of ceramic materials by X-ray fluorescence spectrometry. *Analytical Journal of Chemical Society*, **101**(1207), 761–832.

Chavez G.J. &. Johns W.D. (1995) Mineralogical and ceramic properties of refractory clays from central Missouri (USA). *Applied Clay Science*, **9**, 407–424.

Chen C.Y., Lan G.S. & Tuan W.H. (2000) Microstructural evolution of mullite during the sintering of kaolin powder compacts. *Ceramics International*, **26**, 715–720.

Djangang C.N., Elimbi A., Melo V.C., Lecomte G.L., Nkoumbou C., Soro J., Bonnet J.P., Blanchart P. &

https://doi.org/10.1180/clm.2018.32 Published online by Cambridge University Press

Njopwouo D. (2007) Characteristics and ceramic properties of clays from Mayoum deposit (west Cameroon). *Ceramics International*, **33**(4), 79–88.

Djangang C.N., Elimbi A., Melo V.C., Lecomte G.L., Nkoumbou C., Soro J., Bonnet J.P., Blanchart P. & Njopwouo D. (2008) Sintering of clay–chamotte ceramic composites for refractory bricks. *Ceramics International*, **34**, 1207–1213.

Djangang C.N., Lecomte G.L., Elimbi A., Blanchart P. & Njopwouo D. (2010) Elaboration des céramiques poreuses à base de sciure de bois. *Anales de Chimie*, **35**, 1–16.

El Yacoubi N., Aberkan M. & Ouadia M. (2006) Potentialité d'utilisation d'argiles marocaines de Jbel Kharrou dans l'industrie céramique. *Compte Rendus Geoscience*, **338**, 693–702.

Gualtieri A. & Bertolani M. (1992) Mullite and cristobalite formation in fired products starting from halloysitic clay. *Applied Clay Science*, **7**, 251–262.

ISO 10081-1 (2003) *Classification of Dense Shaped Refractory Products – Part 1: Alumina–Silica*.

Jouenne C.A. (1984) *Traité de Céramiques et Matériaux Minéraux*. Septima, Paris.

Jourdain A. (1966) *Technologie des Produits Céramiques Réfractaires*. Edition, Paris, France.

Kolli M., Hamidouche M., Fantozzi G. & Chevalier J. (2007) Elaboration and characterization of a refractory based on Algerian kaolin. *Ceramics International*, **33**, 1435–1443.

Lapoujade P. & Le Mat Y. (1986) *Traité Pratique sur l'Utilisation des Produits Réfractaires*. Edition, Dourdan, France.

Kornmann M. & Ingénieurs du Centre Technique des Tuiles et Briques (2005) *Matériaux de Construction en Terre Cuite, Fabrication et Propriétés*. Editions Septima, Paris.

Njoya A., Nkoumbou C., Grosbois C., Njopwouo D., Njoya D., Courtin N.A., Yvon J. & Martin F. (2006) Genesis of Mayouom kaolin deposit (west Cameroon). *Applied Clay Science*, **32**, 125–140.

Njoya A. (2007) *Etude du Gisement de Kaolin de Mayouom (Ouest-Cameroun): Cartographie, Minéralogie et Géochimie*. PhD doctoral thesis, Université de Yaoundé I, Yaoundé, Cameroon.

Nkalih M.A. (2016) *Cartographie et Propriétés Physico-Chimiques des Argiles de Foumban (Ouest-Cameroun)*, PhD doctoral thesis, Université de Yaoundé I, Yaoundé, Cameroon.

Nkalih M.A., Njoya A., Yongue F.R., Tapon N.A., Nzeukou N.A., Mache J.R., Siniapkine S., Flament P., Melo C.U., Ngono A. & Fagel N. (2015) Kaolin occurrence in Koutaba (west-Cameroon): Mineralogical and physicochemical characterization for ceramic products. *Clay Mineral*, **50**, 593–606.

Pialy P., Tessier D.N., Njopwouo D. & Bonnet J.P. (2009) Effects of densification and mullitization on the evolution of the elastic properties of a clay-based material during firing. *Journal of the European Ceramic Society*, **29**, 1579–1586.

Poirier J. (2011) Les céramiques réfractaires de l'élaboration aux propriétés d'emploi. *Verres Ceramiques & Composites*, **1**(2), 28–42.

Reynolds R.C. & Moore D.M. (1989) *Principles and Techniques of Quantitative Analysis of Clay Minerals by X-Ray Powder Diffraction*. Oxford University Press, New York.

Ribeiro M.J., Tulyagavov D.U., Ferreira J.M. & Labrincha J.A. (2005) High temperature mullite dissolution in ceramic bodies derived from Al-rich sludge. *Journal of the European Ceramic Society*, **25**, 703–710.

Routschka G. (2004) *Refractory Materials*. 2nd Edition, Vulkan-Verlag, Essen, Germany.

Routschka G. & Wuthnow H. (2012) *Handbook of Refractory Materials*. 4th Edition, Vulkan-Verlag, Essen, Germany.

Sadik C., El Amrani I. & Albizane A. (2014) Recent advances in silica–alumina refractory: a review. *Journal of Asian Ceramic Societies*, **2**, 83–96.

Sahnoune F., Chegaar M., Saheb N., Goeuriot P. & Valdivieso F. (2008) Algerian kaolinite used for mullite formation. *Applied Clay Science*, **38**, 304–310.

Seynou M., Flament P., Sawadogo M., Tirlocq J. & Ouedraogo R. (2013) Formulation de briques réfractaires à base de matières premières kaolinitiques de Tikaré (Burkina Faso). *Journal de la Société Ouest-Africaine de Chimie*, **35**, 49–56.

Staphen C.C. & Gordon L.B. (1992) *Handbook of Industrial Refractories Technology: Principles, Types, Properties and Applications*. 1st Edition. William Andrew, Norwich, NY.

Tassongwa B., Nkoumbou C., Njoya D., Njoya A., Tchop J.L., Yvon J. & Njopwouo D. (2014) Geochemical and mineralogical characteristics of the Mayouom kaolin deposit, west Cameroon. *Earth Science Research*, **3**(1), 14.

Tchamba A.B., Melo U.C., Yongue R. & Njopwouo D. (2011) Phase and microstructure evolution during densification of bauxite of Haleo-Danielle (Minim-Martap, Cameroon) between 1000 and 1600°C. *International Journal of Materials Science*, **6**(1), 89–100.

Zerbo L., Sorgho B., Kam S., Soro J., Millogo Y., Guel B., Traoré K., Gomina M. & Blanchart P. (2012) Comportement thermique de céramiques à base d'argiles naturelles du Burkina Faso. *Journal de la Société Ouest-Africaine de Chimie*, **34**, 48–56.

https://doi.org/10.1180/clm.2018.32 Published online by Cambridge University Press